Image Cover Sheet

CLASSIFICATION	SYSTEM NUMBER
UNCLASSIFIED	151186

TITLE

PE APPROXIMATIONS FOR SCATTERING FROM A ROUGH SURFACE

System Number:

Patron Number:

Requester:

Notes:

DSIS Use only:

Deliver to: TC

DEFENCE RESEARCH ESTABLISHMENT PACIFIC

Research and Development Branch
Department of National Defence

Canada

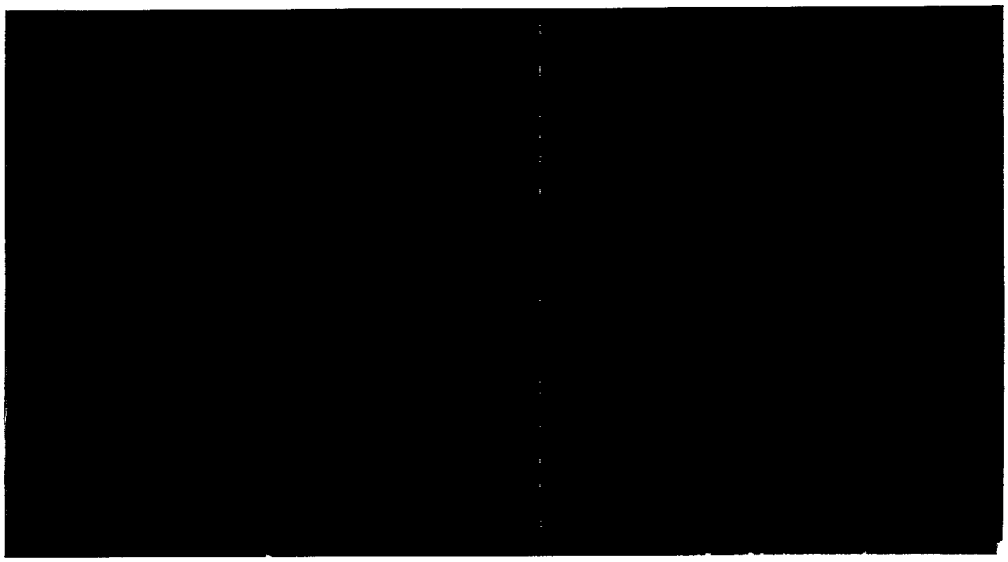

Defence Research Establishment Pacific
Centre de recherches pour la défense pacifique

DEFENCE RESEARCH ESTABLISHMENT PACIFIC

CFB Esquimalt, FMO Victoria, B.C. V0S 1B0

Technical Memorandum 95–21

PE APPROXIMATIONS FOR SCATTERING FROM A ROUGH SURFACE

D.J. THOMSON, G.H. BROOKE† & E.S. HOLMES‡

March 1995

†Numerical Decisions Group, Inc., 917 Fort Street, Suite 8A
Victoria, B.C. V8V 3K3
‡Integrated Performance Decisions, Century Building, Suite 1250
2341 Jefferson Highway, Arlington, VA 22202

Approved By:

Chief DREP

Research and Development Branch
Department of National Defence

Canada

Abstract

Two methods are presented for incorporating the effects of rough boundaries into propagation models based on the parabolic equation (PE) approximation. In particular, the acoustic scattering by a deterministically-rough, pressure-release surface is considered. In the first method, the vertical extent of the computational cell adjacent to the rough boundary is allowed to vary with range. This non-standard grid approach can readily be incorporated into existing finite-difference PE codes. In the second method, a low-impedance air-layer backing is appended to the rough surface and the original rough-surface scattering problem is replaced by one involving scattering from an internal, water/air interface. In this case, both finite-difference and split-step marching algorithms can be accommodated. Numerical results for the forward-scattered component of the field are provided for two benchmark problems.

1. Introduction

In this paper, two PE-based methods are presented for modelling the coherent, forward-scattered component of a wavefield that has interacted with a deterministic rough surface. The motivation for this work was provided by the particular rough-surface configuration that appeared as Test Case 1 of the Reverberation and Scattering Workshop held during 2–6 May, 1994 in Gulfport, MS. We compare our results for this test case, which were computed using standard split-step and/or finite-difference PE algorithms, to reference solutions obtained using a boundary integral equation method.[1,2] In addition to these comparisons, we also re-examine the ASA penetrable wedge problem[3] which we solve using the PE in the context of the second method described herein.

Previous work on incorporating rough-surface scattering from deterministic boundaries into models based on the the parabolic approximation focused on the narrow-angle split-step PE. Dozier,[4] for example, applied conformal mapping techniques in order to locally "flatten" the sea surface before each range step. In contrast, Tappert and Nghiem-Phu[5] and later Thorsos *et al.*[6] modified the complex PE "image" field to satisfy the pressure-release boundary condition on each sloping segment of the surface. Both of these approaches can be extended to wider-angle PEs.[7,8] Other methods for introducing the effects of surface roughness into PE codes have adopted a stochastic viewpoint. For example, Moore-Head *et al.*[9] implemented a localized FFT near the surface to determine the vertical wavenumber spectrum there and then made use of ray theory concepts to map wavenumbers into equivalent grazing angles. In this manner, attenuation could be introduced using a simple loss-versus-angle curve for a given sea-surface roughness. This method allows range steps larger than fractions of a surface wavelength and has been implemented in the US Navy standard PE model to account for rough-surface losses suffered by the coherent part of the field. Recently, Schneider[10] examined some of the numerical approximations that underly this approach and demonstrated its capability for modeling both forward- and backscattered fields in practical applications. Alternatively, Dozier *et al.*[11] describe an extension that accounts for out-of-plane scattering associated with the incoherent component of the field. Stochastic losses due to roughness can also be accommodated through the introduction of special boundary conditions. Collins and Chin-Bing[12,13] used an approximate expansion of the plane-wave reflection coefficient at low angles to model rough-surface effects in terms

of a local boundary condition. On the other hand, the use of non-local, impedance-type boundary conditions can, in principle, account for these coherent scattering losses exactly.[14]

In contrast to the above methods, we describe two techniques that can be introduced into existing PE codes with little programming effort. Our first technique is applicable only to finite-difference-based PEs and involves a straightforward adjustment of the top row of coefficients of the corresponding tri-diagonal matrix representation of the propagator. Essentially, a non-uniform grid is allowed at the top of the PE computational mesh in order to track the variable-height surface as a function of range. A variant of this approach is to impose a higher-order boundary condition along the surface (in addition to the vanishing of the field there) that makes use of the slope of the boundary at each range step. While this higher-order boundary condition is especially important for penetrable rough-bottom applications,[15] its advantage is not as significant for the pressure-release boundary condition under consideration. Finally, for general rough-surface calculations, we suggest a second simple technique whereby the vacuum region above the sea-surface is replaced with a low-impedance fluid, e.g., air. The large impedance mismatch between air and water results in nearly perfect reflection of the field of a water-borne source and, for numerical purposes, allows the rough-surface interface to be treated as an internal boundary. This approach can be adapted to any existing PE code and solution procedure.

The rest of the paper is organized as follows. First, we review the underlying PE theory for both finite-difference and split-step solution algorithms. Then, we describe how finite-difference codes can be modified to handle a range-dependent, variable-depth mesh spacing near the surface of the PE grid. Next, we describe how appending an air-layer backing to the rough surface transforms the given problem of scattering from a variable-depth, pressure-release boundary to scattering from a non-flat internal interface (involving water and air). We compare our PE-based numerical results with reference boundary integral equation solutions generated for the specific rough-surface, scattering configuration introduced at the Reverberation and Scattering Workshop. Finally, we use this air-layer method to re-cast the geometry of the ASA benchmark wedge problem to obtain "2-way PE" results. In contrast to previous work,[16] the use of an air layer allows one to rotate coordinates without introducing any extra bookkeeping effort as the number of depth-grid mesh points remains constant.

2. Theory

2.1. *PE Background*

For a range-independent acoustic medium, the 2D Helmholtz equation in rectangular coordinates (r, z) (z positive down) for the total pressure p can be decomposed into two uncoupled factors representing outgoing and incoming wave-fields with respect to the horizontal range r. In this case, the outgoing component can be recovered from the reduced field ψ that satisfies the two-dimensional evolution equation[17,18]

$$\frac{\partial \psi}{\partial r} = ik_0(Q-1)\psi. \tag{2.1}$$

Over the interval Δr, Eq. (2.1) has the formal solution

$$\psi(r+\Delta r, z) = \exp\{ik_0\Delta r(Q-1)\}\psi(r,z). \tag{2.2}$$

In Eqs. (2.1) and (2.2), $k_0 = 2\pi f/c_0$ is a reference wavenumber and Q denotes the pseudo-differential square-root operator defined by

$$Q = \sqrt{1+\varepsilon+\mu'}, \tag{2.3}$$

where the operators ε and μ' are defined by

$$\begin{aligned} \varepsilon &= N^2 - 1, \\ \mu' &= k_0^{-2}\rho\frac{\partial}{\partial z}\left(\rho^{-1}\frac{\partial}{\partial z}\right). \end{aligned} \tag{2.4}$$

Here, $N = n + i\alpha/k_0$ where $n = c_0/c$ is the refractive index and ρ, c and α denote the density, sound speed and absorption, respectively. The reduced field ψ is related to p by

$$\psi(r,z) = p(r,z)\exp(-ik_0 r)\sqrt{k_0 r}. \tag{2.5}$$

In the case of weakly range-dependent media, Eq. (2.2) can still be applied provided the commutator $[\partial/\partial r, ik_0Q]\psi$, which arises when $Q = Q(r)$, is sufficiently small.

Efficient computational schemes for evaluating the propagator in Eq. (2.2) are obtained by making approximations to the operator Q. For finite-difference approaches, the Padé series expansion[19]

$$Q - 1 \approx \sum_{j=1}^{J} \frac{a_{j,J}(\varepsilon+\mu')}{1+b_{j,J}(\varepsilon+\mu')}, \tag{2.6}$$

where the coefficients $a_{j,J}$ and $b_{j,J}$ are given by

$$\begin{aligned} a_{j,J} &= \frac{2}{2J+1}\sin^2\left(\frac{j\pi}{2J+1}\right), \\ b_{j,J} &= \cos^2\left(\frac{j\pi}{2J+1}\right), \end{aligned} \tag{2.7}$$

leads to the higher-order PE[20]

$$\frac{\partial\psi}{\partial r} = ik_0\sum_{j=1}^{J}\frac{a_{j,J}(\varepsilon+\mu')}{1+b_{j,J}(\varepsilon+\mu')}\psi. \tag{2.8}$$

Using the method of fractional steps, Eq. (2.8) can be solved at each range step as a sequence of J systems of equations, where the jth system is given by

$$[1+b_{j,J}(\varepsilon+\mu')]\frac{\partial\psi_j}{\partial r} = ik_0 a_{j,J}(\varepsilon+\mu')\psi_j. \tag{2.9}$$

The Crank-Nicolson procedure for solving Eq. (2.9) (see e.g., Lee and McDaniel[21]) makes use of the approximations

$$\begin{aligned} \frac{\partial \psi_j}{\partial r} &\approx \frac{\psi(r+\frac{j}{J}\Delta r, z) - \psi(r+\frac{j-1}{J}\Delta r, z)}{\Delta r}, \\ \psi_j &\approx \frac{\psi(r+\frac{j}{J}\Delta r, z) + \psi(r+\frac{j-1}{J}\Delta r, z)}{2}, \end{aligned} \tag{2.10}$$

to yield, for $j = 1, \ldots, J$,

$$\left[1 + c^-_{j,J}(\varepsilon + \mu')\right] \psi(r+\tfrac{j}{J}\Delta r, z) = \left[1 + c^+_{j,J}(\varepsilon + \mu')\right] \psi(r+\tfrac{j-1}{J}\Delta r, z), \tag{2.11}$$

where we have set $c^{\pm}_{j,J} = b_{j,J} \pm \frac{1}{2} i k_0 \Delta r a_{j,J}$. If the derivative term $\mu'\psi$ is evaluated using the heterogeneous approximation[22]

$$\mu'\psi(r,z) \approx \frac{\rho_-\psi(r, z-\Delta z) - \rho_0\psi(r,z) + \rho_+\psi(r, z+\Delta z)}{k_0^2 \Delta z^2}, \tag{2.12}$$

where $\rho_\pm$ and ρ_0 denote the density combinations

$$\begin{aligned} \rho_\pm &= \frac{2\rho(r,z)}{\rho(r,z) + \rho(r, z \pm \Delta z)}, \\ \rho_0 &= \rho_- + \rho_+, \end{aligned} \tag{2.13}$$

then Eq. (2.11) becomes a tri-diagonal system of equations that can be solved efficiently by double recursion. For numerical reasons, it is convenient in some applications to replace the real coefficients $a_{j,J}$ and $b_{j,J}$ in Eq. (2.7) with complex ones. For $J \leq 7$, suitable values have been determined numerically and tabulated by Collins.[23]

In order to handle density variations in the context of the split-step algorithm, it is necessary to modify Q in the above development. The change of variable $\tilde{\psi} = \sqrt{\rho}\psi$ transforms Eq. (2.2) into

$$\tilde{\psi}(r + \Delta r, z) = \exp\{ik_0 \Delta r(\tilde{Q} - 1)\}\tilde{\psi}(r, z), \tag{2.14}$$

where the square-root operator $\tilde{Q}$ is defined by

$$\tilde{Q} = \sqrt{1 + \varepsilon' + \mu} \tag{2.15}$$

and

$$\begin{aligned} \varepsilon' &= \varepsilon + \frac{1}{2k_0^2}\sqrt{\rho}\frac{\partial}{\partial z}\left(\frac{1}{\rho\sqrt{\rho}}\frac{\partial \rho}{\partial z}\right), \\ \mu &= k_0^{-2}\frac{\partial^2}{\partial z^2}. \end{aligned} \tag{2.16}$$

With this maneuver, density variations result in terms added to ε to produce an effective index of refraction $\tilde{N} = \sqrt{1 + \varepsilon'}$. In addition, the cross-derivative operator is simplified, i.e., $\mu' \to \mu$. Because standard geoacoustic density profiles contain step discontinuities and because $\tilde{N}$ contains derivatives of ρ, these regions of the density profile must

be smoothed appropriately.[17] Finally, incorporating the above density modifications, the wide-angle, split-operator approximation to $\tilde{Q}$ given by[22,24,25]

$$\tilde{Q} - 1 \approx -2 + \sqrt{1+\mu} + \sqrt{\varepsilon' - 1} \tag{2.17}$$

leads to the split-step Fourier marching algorithm[26]

$$\tilde{\psi}(r + \Delta r, z) \approx \tag{2.18}$$

$$\exp\left\{ik_0 \Delta r(\tilde{N} - 2)\right\} \cdot \mathrm{FFT}^{-1}\left[\exp\left\{ik_0 \Delta r \sqrt{1 - k_z^2/k_0^2}\right\} \cdot \mathrm{FFT}\left[\tilde{\psi}(r, z)\right]\right]. \tag{2.19}$$

2.2. *Non-uniform Depth-grid*

In most applications of the PE to underwater sound propagation, the sea-surface is taken to be flat and pressure-release, i.e., $\psi(r, 0) = 0$. Moreover, both finite-difference and split-step marching algorithms are usually restricted to an equi-spaced depth-mesh with spacing Δz. In the present work, the rough surface $z = \zeta(r)$, defined by its vertical displacement from the plane $z = 0$, is taken to have zero mean ($\langle\zeta\rangle = 0$). For finite-difference representations, it is possible to use a non-uniform depth-grid that adjusts with range to the local displacement of the non-flat boundary. The simplest approach, then, one that does not require the number of depth-grid points to change, is to modify only the grid-spacing of the cell adjacent to the surface.

Figure 1 shows a schematic of the geometric configuration for the rough-surface scattering problem. The insert illustrates how the surface is represented in PE calculations by a sequence of range-independent sections. We arrange for the shallowest *interior* mesh point of the PE grid to lie Δz below the deepest portion of the surface which we take to be the plane $z = 0$. This amounts to shifting the rough surface upwards by the distance $H = \max\{\zeta\}$. At the range position I, the uppermost mesh point lies along the plane $z = -h\Delta z$ where $h \geq 0$. Along this locally flat surface, the pressure-release boundary condition requires $\psi(r, -h\Delta z) = 0$. To derive a variable-spaced difference formulation for the PE in the vicinity of the boundary there, we expand the field in a Taylor series to $O(\Delta z^2)$ about the level $z = \Delta z$ to obtain

$$\begin{aligned} \psi(r, -h\Delta z) &\approx \psi(r, \Delta z) - (1+h)\Delta z \psi'(r, \Delta z) + \tfrac{1}{2}(1+h)^2 \Delta z^2 \psi''(r, \Delta z), \\ \psi(r, 2\Delta z) &\approx \psi(r, \Delta z) + \Delta z \psi'(r, \Delta z) + \tfrac{1}{2}\Delta z^2 \psi''(r, \Delta z). \end{aligned} \tag{2.20}$$

Here the prime denotes $\partial/\partial z$. Solving this system for $\psi''(r, \Delta z)$ yields

$$k_0^{-2}\psi''(r, \Delta z) \approx \frac{h_-\psi(r, -h\Delta z) - h_0\psi(r, \Delta z) + h_+\psi(r, 2\Delta z)}{k_0^2 \Delta z^2}, \tag{2.21}$$

where the coefficients $h_\pm$ and h_0 are defined by

$$h_- = \frac{2}{(h+1)(h+2)},$$

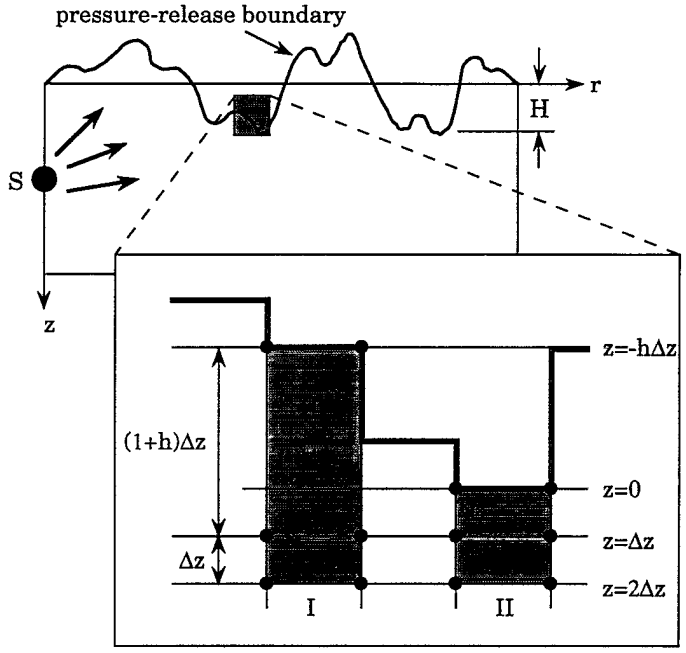

Fig. 1. Configuration for the variable-depth grid method.

$$h_0 = \frac{2}{h+1}, \qquad h_+ = \frac{2}{h+2}. \tag{2.22}$$

Note that at range position II, where $h \to 0$, the coefficients in Eq. (2.22) reduce to the usual centered-difference values for the operator μ. If we consider the density to be uniform near the surface, then it is seen that the effects of a variable-height surface can be accommodated simply by replacing the variable-density coefficients along the top row in Eq. (2.13) with the corresponding spatially-weighted ones in Eq. (2.22).

Two limitations of this method are worth noting. First, by construction, there are no grid points lying between $\min\{\zeta\} < z < \max\{\zeta\}$ and, consequently, no knowledge of the field in this region. Second, the accuracy of the method is expected to degrade when the displacement of the rough surface exceeds some significant fraction of an acoustic wavelength. That is, for a given rough surface, the accuracy should improve as the frequency is reduced.

2.3. *Air-layer Backing*

To overcome the restrictions of the variable-depth grid method, an alternative approach for treating the effect of a rough surface is proposed. It is based on the well-known observation that the large impedance drop across the ocean/air interface ($\approx 2 \cdot 10^{-4}$) results in nearly perfect, out-of-phase reflection of sound for a water-borne source (see, e.g., Chap-

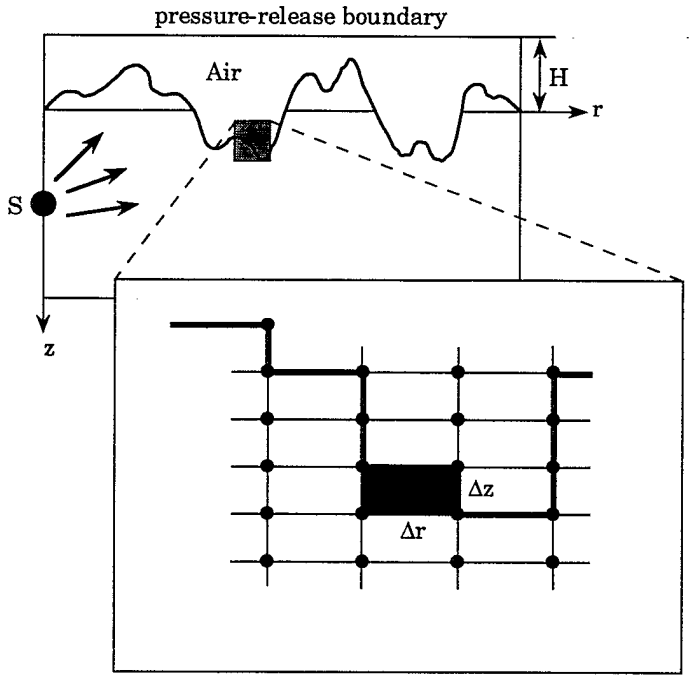

Fig. 2. Configuration for the air-layer backing method.

man et al.[27]). Consequently, most numerical realizations of underwater sound propagation idealize the sea-surface as a pressure-release boundary. This observation suggests that the rough-surface scattering problem be modified by appending a low-impedance air-layer to the region above the boundary. In this way, scattering by an *external* pressure-release boundary is replaced with scattering by an *internal* fluid/fluid interface across which the usual boundary conditions on the acoustic field apply. The underwater reflection coefficient associated with the sea/air boundary should be close to -1. The configuration associated with this approach is illustrated in Fig. (2) for the same rough-surface scenario considered previously. With the addition of an air layer, the standard equi-spaced PE computational grid and solution procedures can be applied to the modified scattering problem. It is only necessary to modify the geoacoustic-profile information that is supplied to the PE code. Moreover, it is worthwhile pointing out that with this approach, values of the field between the keels of the rough surface are available at the resolution of the computational grid.

3. Numerical Results

3.1. *R & S Workshop Rough-surface*

The original, rough-surface, finite-difference PE results that were presented at the Reverberation and Scattering Workshop are shown as the solid curves in Fig. (3) to Fig. (6) for two source frequencies. These results were obtained using $J = 1$ in Eq. (2.8), which cor-

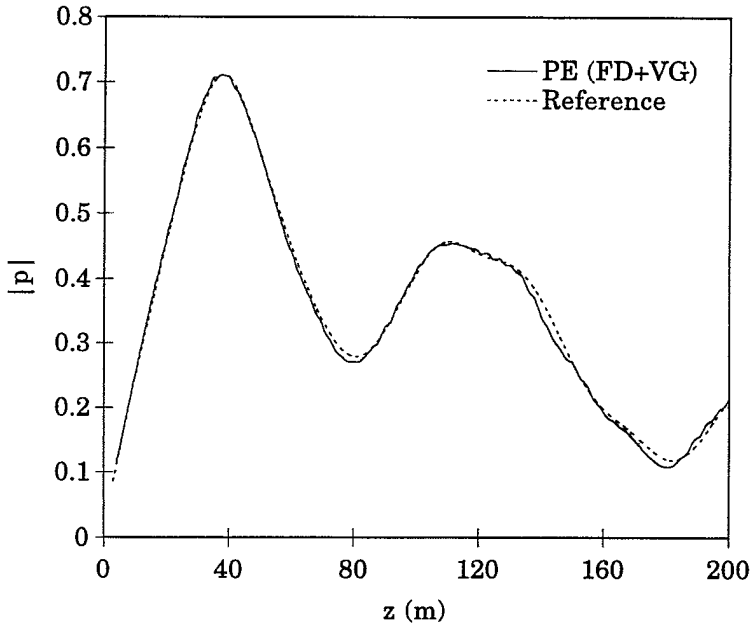

Fig. 3. Finite-difference PE (variable-depth grid) versus reference solution. $f = 100$ Hz.

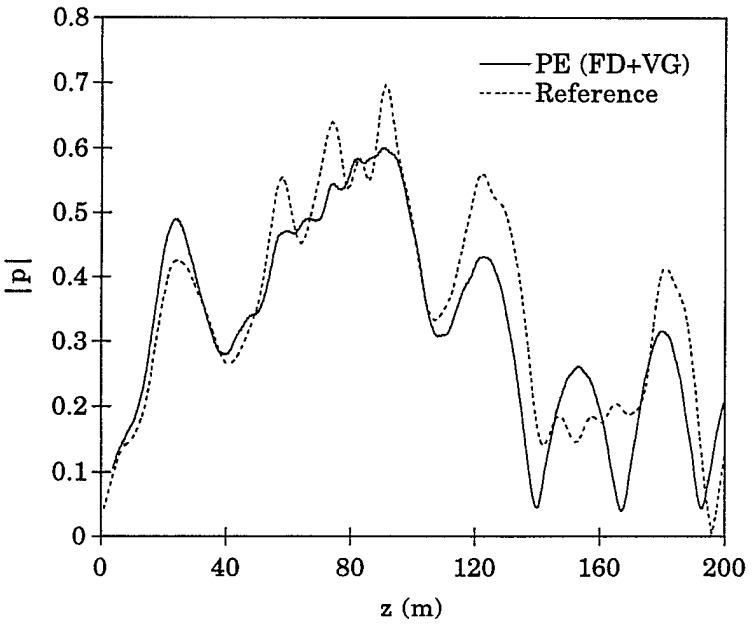

Fig. 4. Finite-difference PE (variable-depth grid) versus reference solution. $f = 400$ Hz.

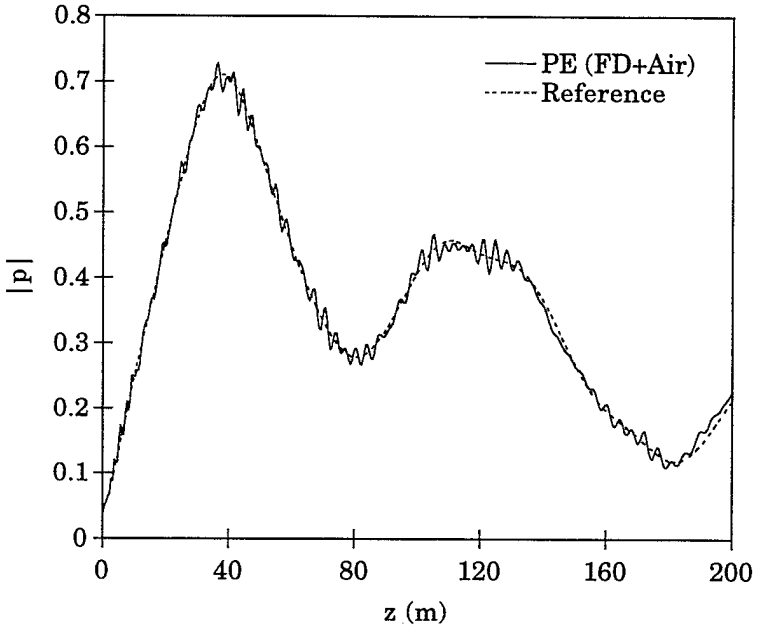

Fig. 5. Finite-difference PE (air-layer backing) versus reference solution. $f = 100$ Hz.

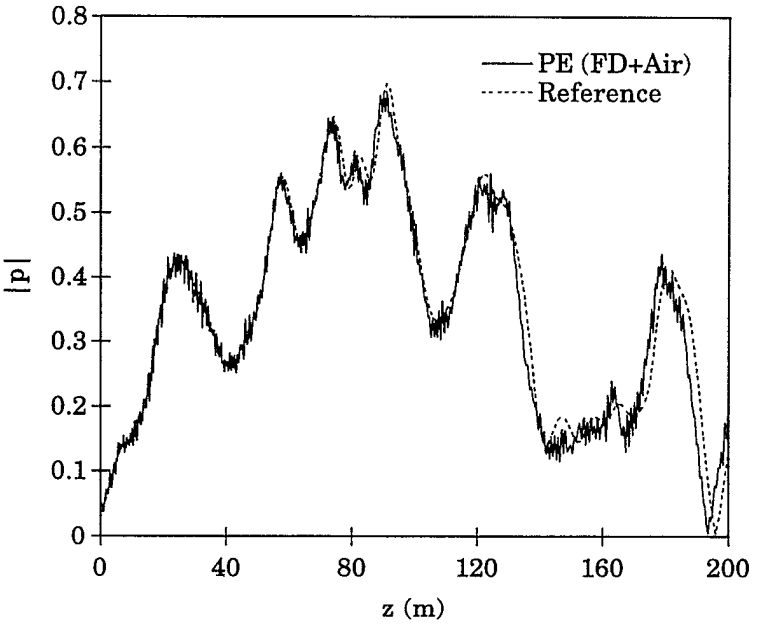

Fig. 6. Finite-difference PE (air-layer backing) versus reference solution. $f = 400$ Hz.

responds to Claerbout's square-root approximation, a range step-size of $\Delta r = 0.375$ m, and depth step-sizes of $\Delta z = 0.5$ m for the 100-Hz source and $\Delta z = 0.25$ m for the 400-Hz source. In addition, a non-local, impedance-type boundary condition developed by Papadakis[28] and implemented by Thomson and Mayfield[29] was used to truncate the computational grid just below the depth of the bottom-most receiver. The use of this non-reflecting boundary condition precluded the need for an absorbing layer to prevent spurious reflections from the base of the PE grid. The dashed, reference curves that are shown in these figures were generated using boundary integral equation techniques.[2]

The variable-depth grid results for 100 Hz are given in Fig. (3) while those for 400 Hz are given in Fig. (4). The 100-Hz PE results agree closely with the reference solution values, although some oscillation is evident. At the lower frequency, the maximum displacement of the rough surface from the plane $z = 0$ is about a half-wavelength. At 400 Hz, the maximum surface displacement is about two wavelengths, and the variable-depth grid results are observed to diverge considerably from the reference values. This disagreement between solutions at the higher frequency motivated the consideration of the air-layer backing method.

The finite-difference results obtained with a 20-m air-layer backing to the rough surface are shown in Fig. (5) and Fig. (6). The values $c = 300$ m s^{-1}, $\rho = 0.0012$ g cm^{-3}, and $\alpha = 0.5$ dB/wavelength were used for air. With this approach, the agreement is good even at 400 Hz, although the rate of the oscillations is greater. Furthermore, there is some alignment mismatch between the PE and reference solutions at the deeper receiver depths. Efforts to reduce the oscillation "noise" by increasing the absorption of the air-layer and by increasing its thickness had no appreciable effect.

During the Workshop, one of the authors (ESH) was able to incorporate the air-layer backing method into a version of the US Navy standard PE model running on a PC notebook computer. This code uses the wide-angle, split-step marching algorithm based on Eq. (2.18). The comparison between these USN PE results and the reference solutions are shown in Fig. (7) and Fig. (8). These calculations were carried out using grid-steps $\Delta z \approx 1$ m and $\Delta r \approx 2$ m and included an absorbing layer in the region $250 < z < 340$ m. Considering the subsampling of the rough surface and the fact that the code is an operational model, the US Navy PE solutions compare very favourably with the reference solutions. This implementation was noteworthy in that it demonstrated a real-time transfer of technology from the research and development community to an operational system.

Subsequent to the workshop, the PE solutions to the rough-surface problem were reworked in an effort to address the "noise" and alignment issues. In order to increase the Padé order in the finite-difference methods, it was necessary to forgo the non-local boundary condition and append a non-physical, absorbing layer to attenuate the downgoing components of the field. For this purpose, a false absorbing region was appended between $256 < z < 512$ m in which the attenuation increased linearly from zero to 10 dB/wavelength. In addition, complex Padé coefficients of order $J = 2$ were used.[23] With these parameters, a slightly smoother solution (not reproduced here) was obtained for the variable-grid finite-difference method. In contrast, for the air-backed layer method, the results shown in Fig. (9) and Fig. (10) indicate that these changes generate significantly improved comparisons with

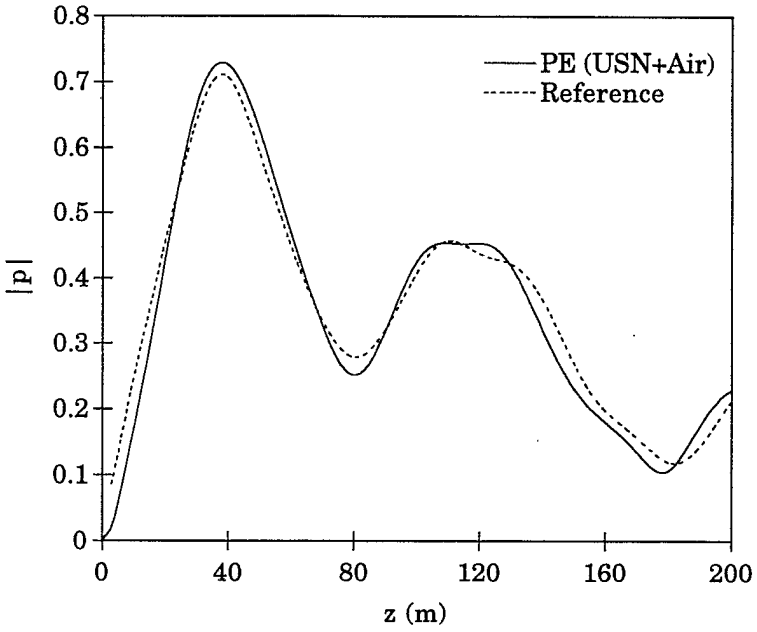

Fig. 7. US Navy standard PE (air-layer backing) versus reference solution. $f = 100$ Hz.

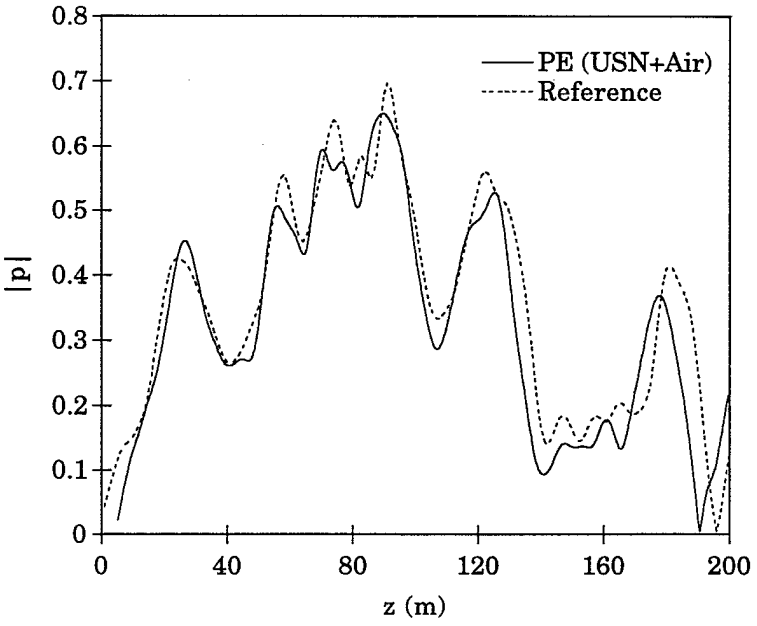

Fig. 8. US Navy standard PE (air-layer backing) versus reference solution. $f = 400$ Hz.

the reference solutions. The higher-order, complex Padé coefficients have eliminated the "noise" and corrected some of the alignment error observed in the previous PE solutions.

Figure (11) and Fig. (12) show the results of applying a research version of the split-step PE code[22] to the rough-surface scattering configuration. These results were generated using the same computational and environmental parameters that were used for the finite-difference calculations of Fig. (9) and Fig. (10). For each frequency, it is apparent that the wide-angle, split-step solution aligns well with the reference solution but suffers a nearly uniform reduction in amplitude. The cause of the discrepancy in level for this algorithm is not known.

3.2. *ASA Benchmark Wedge*

An air-layer backing can also be used in problems involving underwater sound propagation over a sloping bottom. It is now well-known that the standard method of representing a sloping bottom with a sequence of range-independent sections (the staircase model) in PE calculations violates energy-conservation principles.[30] Several techniques have been developed for ameliorating this difficulty.[15,16,31–34] Of these, Collins' rotated PE[16] was shown to result in two-way accuracy for the one-way outgoing component of the field by aligning the computational grid with the plane of the sloping bottom. In rotated coordinates, continuity of pressure and vertical particle velocity are satisfied naturally along the sea-bottom interface just as in a range-independent problem. Although the sea-surface is now represented by a staircase boundary, the vanishing of the field on the horizontal steps, in the limit of small vertical steps, is sufficient to approximate the pressure-release boundary condition everywhere. The rotated PE requires special code, however, to decrease (increase) the number of vertical grid elements as the solution is marched up (down) the slope. By adding an air layer, this special bookkeeping effort can be avoided.

The physical and environmental parameters of the ASA benchmark wedge problem are given in Fig. (13). The configuration with the addition of an air-layer backing and rotated coordinate system is shown in Fig. (14). The (r', z')-system is rotated and translated about the source point $r = 0, z = z_s$. It is convenient to regard r' and z as the independent variables, so that r and z' are determined by

$$\begin{aligned} r + r_0 &= \frac{r' + z \sin\gamma}{\cos\gamma}, \\ z' &= (r + r_0)\sin\gamma + z\cos\gamma. \end{aligned} \tag{3.23}$$

Here, $\gamma = \arctan(.05) \approx 2.86°$ is the wedge angle and $r_0 = z_s/\tan(.05) = 5$ m is the offset along the r-axis. The (r, z')-pairs corresponding to a receiver along $z = $ const. are determined from Eq. (3.23). The transmission loss comparisons between the normal PE, solved in the (r, z)-system, and the rotated PE, solved in the (r', z')-system, are given in Fig. (15) for a receiver at $z_r = 30$ m and in Fig. (16) for the 150-m receiver. A 20-m air layer, a 2-term Padé approximation of the square-root, and the step-sizes $\Delta r' = 5$ m and $\Delta z' = 0.5$ m were used for these finite-difference PE calculations. The PE solutions for the rotated grid do not exhibit the loss of energy observed in the PE solutions for the normal

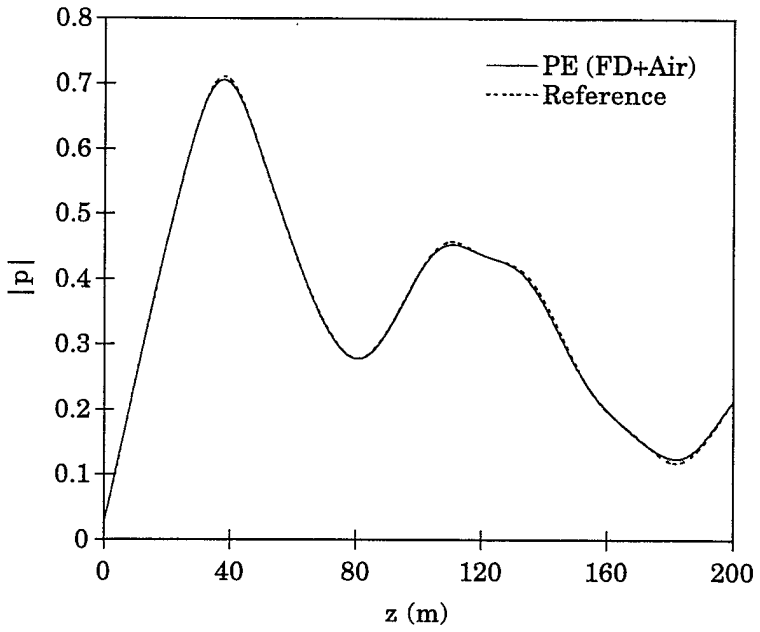

Fig. 9. Finite-difference PE (air-layer backing) versus reference solution. $f = 100$ Hz.

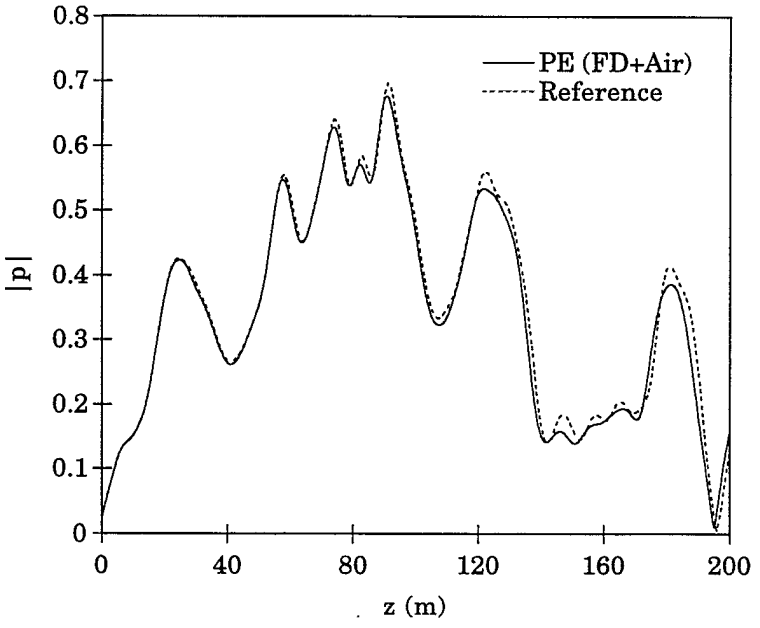

Fig. 10. Finite-difference PE (air-layer backing) versus reference solution. $f = 400$ Hz.

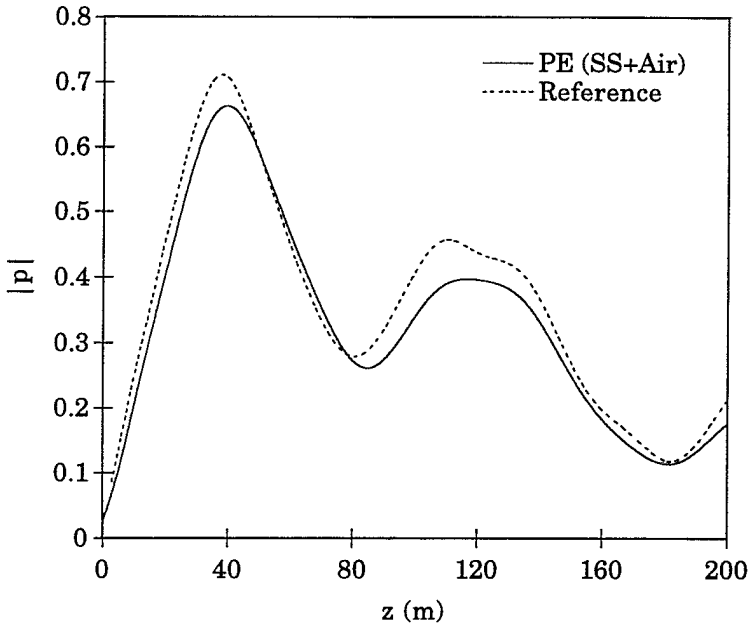

Fig. 11. Split-step PE (air-layer backing) versus reference solution. $f = 100$ Hz.

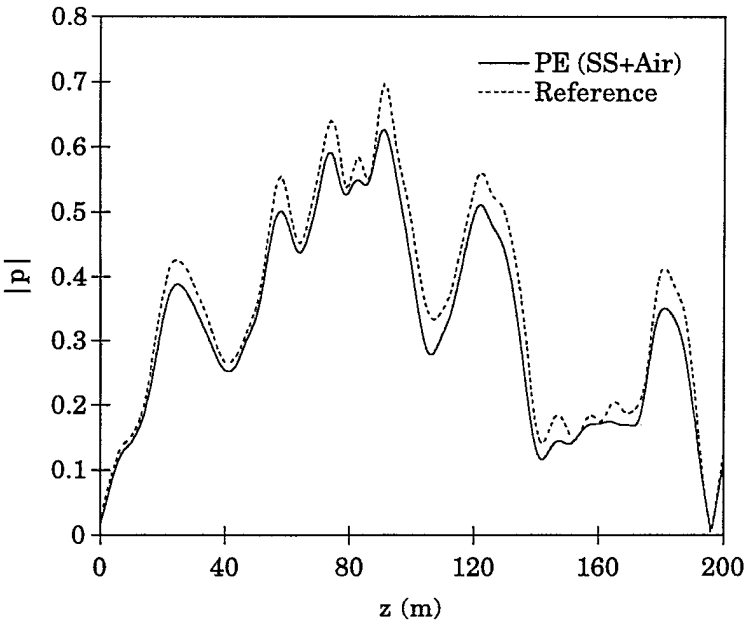

Fig. 12. Split-step PE (air-layer backing) versus reference solution. $f = 400$ Hz.

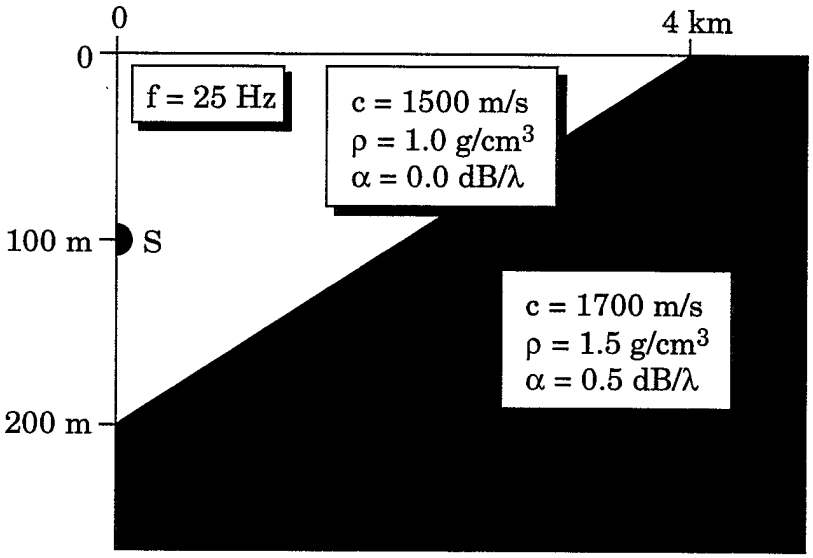

Fig. 13. Physical and environmental parameters for the ASA wedge.

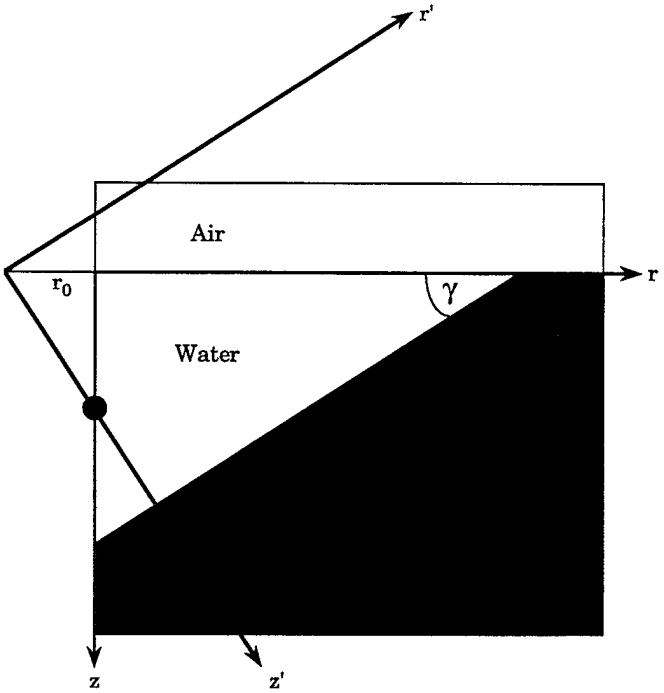

Fig. 14. Rotated coordinate system for the air-layer backed ASA wedge.

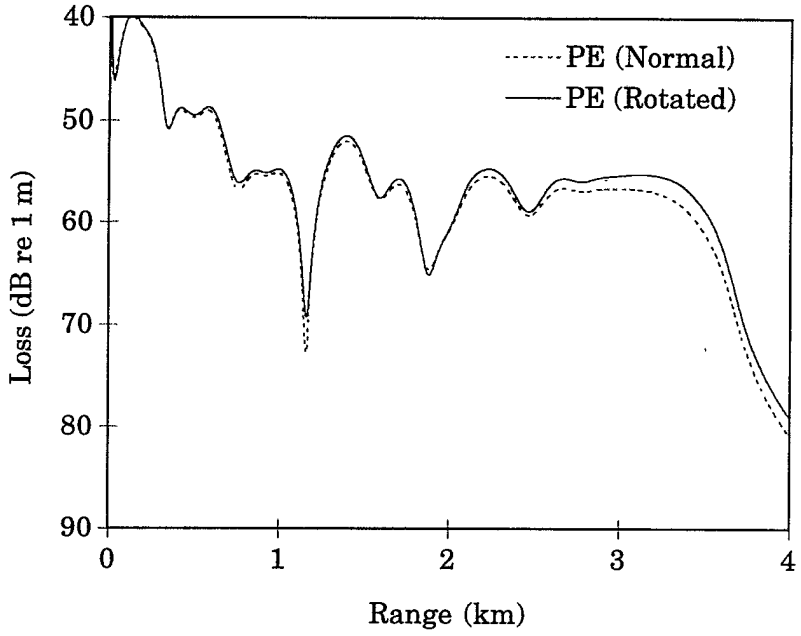

Fig. 15. Normal PE versus rotated PE solutions for the ASA wedge. $z_r = 30$ m.

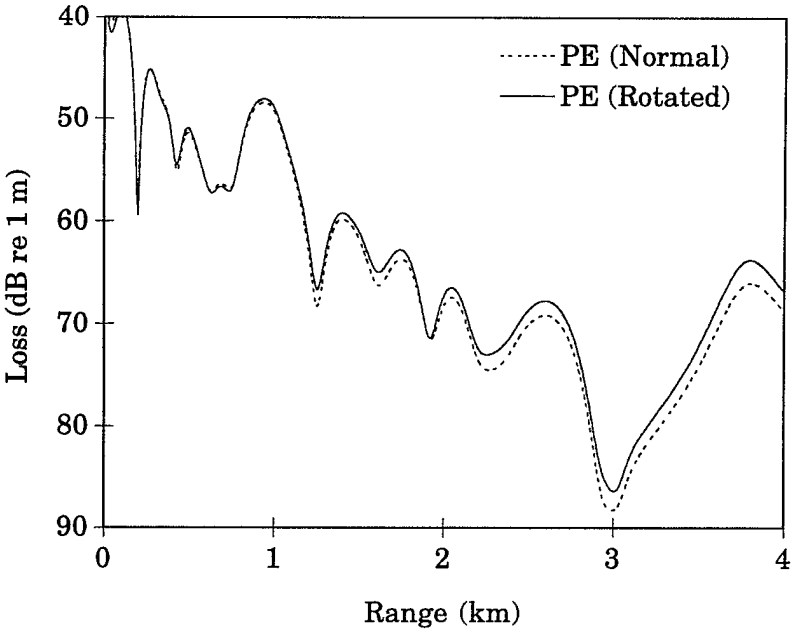

Fig. 16. Normal PE versus rotated PE solutions for the ASA wedge. $z_r = 150$ m.

grid, which uses a staircase representation of the sloping bottom.

4. Conclusions

Two methods for incorporating a deterministic rough-surface into parabolic equation models were described and applied to the particular rough-surface configuration that was offered for numerical consideration at the Reverberation and Scattering Workshop (2–6 May 1994 in Gulfport, MS). The first method, suitable only for finite-difference-based PE models, introduced a variable-depth grid element adjacent to the rough surface to track its displacement as a function of range. This method is limited to rough surfaces whose height variation is sufficiently small relative to an acoustic wavelength. To overcome this restriction, a second method was introduced that involved appending an air-layer backing to the rough surface. In this case, scattering from an external, pressure-release boundary is replaced with scattering from an internal, water/air interface. This approach is applicable to both finite-difference and split-step solution procedures. For the air-layer method, the finite-difference solutions at both frequencies were in excellent agreement with reference solutions based on integral equation techniques whereas the split-step solutions underestimated the peak amplitudes by about 10–15%. The air-layer method was also shown to simplify the calculations associated with the rotated PE method that was developed to handle PE propagation over a sloping ocean-bottom.

Acknowledgements

We are grateful to Eric Thorsos for providing the 100-Hz reference solution for the rough-surface scattering problem in response to our request. This allowed us to evaluate the dependence of the variable-grid method on source wavelength, and inspired us to examine the air-backed layer approach.

References

1. E.I. Thorsos, "Acoustic scattering from a "Pierson-Moskowitz" sea surface," J. Acoust. Soc. Am. **88**, 335–349 (1990).
2. E.I. Thorsos, "Boundary integral equation solution for test case I," presented at the Reverberation and Scattering Workshop, 2–6 May 1994, Gulfport, MS.
3. F.B. Jensen and C.M. Ferla, "Numerical solutions of range-dependent benchmark problems in ocean acoustics," J. Acoust. Soc. Am. **87**, 1499–1510 (1990).
4. L.B. Dozier, "PERUSE: A numerical treatment of rough surface scattering for the parabolic wave equation," J. Acoust. Soc. Am. **75**, 1415–1432 (1984).
5. F.D. Tappert and L. Nghiem-Phu, "A new split-step Fourier algorithm for solving the parabolic wave equation with rough surface scattering," J. Acoust. Soc. Am. Suppl. 1 **77**, S101 (1985).
6. E.I. Thorsos, J.W. Ballard and T.E. Ewart, "Rough surface scattering with the parabolic wave equation using a split-step method," J. Acoust. Soc. Am. Suppl. 1 **84**, S220–S221 (1988).
7. K.B. Smith and F.D. Tappert, "The University of Miami Parabolic Equation Model," Marine Physical Laboratory, Scripps Institution of Oceanography, MPL Tech. Memo. 432, May 1993.
8. G.V. Norton, J.C. Novarini and R.S. Keiffer, "Inclusion of rough surface scattering in a finite-element parabolic equation model," presented at the Reverberation and Scattering Workshop, 2–6 May 1994, Gulfport, MS.

9. M.E. Moore-Head, W. Jobst and E.S. Holmes, "Parabolic equation modeling with angle-dependent surface loss," J. Acoust. Soc. Am. **86**, 247–251 (1989).
10. H.G. Schneider, "Surface loss, scattering, and reverberation with the split-step parabolic equation model," J. Acoust. Soc. Am. **93**, 770–781 (1993).
11. L.B. Dozier, J.S. Hanna and C.R. Pearson, "Treatments of incoherent scattering for the parabolic equation and ASTRAL propagation models," in *Ocean Variability and Acoustic Propagation*, edited by J. Potter and A. Warns-Varnas (Kluwer, The Netherlands, 1991), pp. 265–281.
12. M.D. Collins and S.A. Chin-Bing, "Three-dimensional sound propagation in shallow water including the effects of rough surfaces," in *Computational Acoustics, Volume* 3, edited by D. Lee, A. Cakmak and R. Vichnevetsky (Elsevier, North-Holland, 1990), pp. 247–259.
13. M.D. Collins and S.A. Chin-Bing, "A three-dimensional parabolic equation model that includes the effects of rough boundaries," J. Acoust. Soc. Am. **87**, 1104–1109 (1990).
14. M.E. Mayfield, "Nonreflective boundary conditions for Schroedinger's equation," Univ. of Rhode Island, Kingston, RI, Ph.D Thesis, 1989.
15. G.H. Brooke, D.J. Thomson and P. Wort, "A Sloping-boundary condition for efficient PE calculations in range-dependent acoustic media," submitted to J. Comp. Acoust.
16. M.D. Collins, "The rotated parabolic equation and sloping ocean bottoms," J. Acoust. Soc. Am. **87**, 1035–1037 (1990).
17. F.D. Tappert, "The parabolic approximation method," in *Wave Propagation and Underwater Acoustics*, edited by J.B. Keller and J.S. Papadakis (Springer, New York, 1977), Chap. 5, pp. 224–287.
18. J.A. Davis, D. White, and R.C. Cavanagh, "NORDA Parabolic Equation Workshop, 31 March–3 April 1981," Tech. Note 143, Naval Ocean Research and Development Activity, NSTL Station, MS, 1982.
19. A. Bamberger, B. Enguist, L. Halpern and P. Joly, "Higher order paraxial wave equation approximations in heterogeneous media," SIAM J. Appl. Math **48**, 129–154 (1988).
20. M.D. Collins, "Benchmark calculations for higher-order parabolic equations," J. Acoust. Soc. Am. **87**, 1535–1538 (1990).
21. D. Lee and S.T. McDaniel, "Ocean acoustic propagation by finite-difference methods," Comput. Math. Applic. **14**, 305–423 (1987).
22. D.J. Thomson, "Wide-angle parabolic equation solutions to two range-dependent benchmark problems," J. Acoust. Soc. Am. **87**, 1514–1520 (1990).
23. M.D. Collins, "Higher-order Padé approximations for accurate and stable elastic parabolic equations with application to interface wave propagation," J. Acoust. Soc. Am. **89**, 1050–1057 (1991).
24. M.D. Feit and J.A. Fleck, "Light propagation in graded-index optical fibers," Appl. Optics **17**, 3990–3998 (1978).
25. D.J. Thomson and N.R. Chapman, "A wide-angle split-step algorithm for the parabolic equation," J. Acoust. Soc. Am. **74**, 1848–1854 (1983).
26. F.D. Tappert and R.H. Hardin, "Computer simulation of long-range ocean acoustic propagation using the parabolic equation method," in *Proceedings of the 8th International Congress on Acoustics* (Goldcrest, London, 1974), Vol. 2, p. 452.
27. D.M.F. Chapman, D.J. Thomson and D.D. Ellis, "Modeling air-to-water sound transmission using standard numerical codes of underwater acoustics," J. Acoust. Soc. Am. **91**, 1904–1910 (1992).
28. J.S. Papadakis, "Impedance formulation of the bottom boundary condition for the parabolic equation model in underwater acoustics," in J.A. Davis, D. White and R.C. Cavanagh, *NORDA Parabolic Equation Workshop, 31 March–3 April, 1981*, Naval Ocean Research and Development Activity, NSTL Station, MS, Tech. Note 143 (1982), p. 83.
29. D.J. Thomson and M.E. Mayfield, "An exact radiation condition for use with the *a posteriori* PE method," J. Comp. Acoust. **2**, 113–132 (1994).

30. M.B. Porter, F.B. Jensen and C.M. Ferla, "The problem of energy conservation in one-way models," J. Acoust. Soc. Am. **89**, 1058–1067 (1991).
31. M.D. Collins and E.K. Westwood, "A higher-order energy-conserving parabolic equation for range-dependent ocean depth, sound speed and density," J. Acoust. Soc. Am. **89**, 1068–1075 (1991).
32. M.D. Collins and R.B. Evans, "A two-way parabolic equation for acoustic backscattering in the ocean," J. Acoust. Soc. Am. **91**, 1357–1368 (1992).
33. G.H. Brooke and D.J. Thomson, "A single-scatter formalism for improving PE calculations in range-dependent media," in *PE Workshop II: Proceedings of the Second Parabolic Equation Workshop*, edited by S.A. Chin-Bing, D.B. King, J.A. Davis and R.B. Evans (US Government Printing Office, Washington, D.C., 1993), pp. 126–144.
34. M.D. Collins, "Higher-order, energy-conserving, two-way, and elastic parabolic equations," in *PE Workshop II: Proceedings of the Second Parabolic Equation Workshop*, edited by S.A. Chin-Bing, D.B. King, J.A. Davis and R.B. Evans (US Government Printing Office, Washington, D.C., 1993), pp. 145–168.

Title:	PE Approximations for Scattering from a Rough Surface
Authors:	D.J. Thomson, G.H. Brooke and E.S. Holmes
Report Series:	Technical Memorandum 95–21
Date:	March 1995
Classification:	Unclassified

Distribution List:

1 – DSIS

1 – DREA

29 – DREP

- D.J. Thomson (10)
- G.H. Brooke (6)
- E.S. Holmes (6)
- J.M. Ozard (1)
- J.S. Kennedy (1)
- N.R. Chapman (1)
- G.R. Ebbeson (1)
- B.H. Maranda (1)
- G.J. Heard (1)
- M.L. Yeremy (1)

UNCLASSIFIED

SECURITY CLASSIFICATION OF FORM
(highest classification of Title, Abstract, Keywords)

DOCUMENT CONTROL DATA

(Security classification of title, body of abstract and indexing annotation must be entered when the overall document is classified)

1 ORIGINATOR (the name and address of the organization preparing the document. Organizations for whom the document was prepared, e.g. Establishment sponsoring a contractor's report, or tasking agency, are entered in section 8.)

Defence Research Establishment Pacific
FMO Victoria, B.C. V0S 1B0

2. SECURITY CLASSIFICATION (overall security classification of the document including special warning terms if applicable)

Unclassified

3. TITLE (the complete document title as indicated on the title page. Its classification should be indicated by the appropriate abbreviation (S,C or U) in parentheses after the title.)

PE Approximations for Scattering from a Rough Surface (U)

4 AUTHORS (Last name, first name, middle initial)

Thomson, David J., Brooke, Gary H., Holmes, Eleanor S.

5 DATE OF PUBLICATION (month and year of publication of document)	6a. NO. OF PAGES (total containing information. Include Annexes, Appendices, etc.)	6b. NO. OF REFS (total cited in document)
March 1995	20	34

7 DESCRIPTIVE NOTES (the category of the document, e.g. technical report, technical note or memorandum. If appropriate, enter the type of report, e.g. interim, progress, summary, annual or final. Give the inclusive dates when a specific reporting period is covered.)

Technical Memorandum

8. SPONSORING ACTIVITY (the name of the department project office or laboratory sponsoring the research and development. Include the address.)

Defence Research Establishment Pacific
FMO Victoria, B.C. V0S 1B0

9a. PROJECT OR GRANT NO. (if appropriate, the applicable research and development project or grant number under which the document was written. Please specify whether project or grant)	9b. CONTRACT NO. (if appropriate, the applicable number under which the document was written)
DRDM 08	

10a. ORIGINATOR'S DOCUMENT NUMBER (the official document number by which the document is identified by the originating activity. This number must be unique to this document.)	10b. OTHER DOCUMENT NOS. (Any other numbers which may be assigned this document either by the originator or by the sponsor)
95-21	

11. DOCUMENT AVAILABILITY (any limitations on further dissemination of the document, other than those imposed by security classification)

- (X) Unlimited distribution
- ( ) Distribution limited to defence departments and defence contractors; further distribution only as approved
- ( ) Distribution limited to defence departments and Canadian defence contractors; further distribution only as approved
- ( ) Distribution limited to government departments and agencies; further distribution only as approved
- ( ) Distribution limited to defence departments; further distribution only as approved
- ( ) Other (please specify):

12. DOCUMENT ANNOUNCEMENT (any limitation to the bibliographic announcement of this document. This will normally correspond to the Document Availability (11). However, where further distribution (beyond the audience specified in 11) is possible, a wider announcement audience may be selected.)

UNCLASSIFIED

SECURITY CLASSIFICATION OF FORM

DCD03 2/06/87

13. ABSTRACT (a brief and factual summary of the document. It may also appear elsewhere in the body of the document itself. It is highly desirable that the abstract of classified documents be unclassified. Each paragraph of the abstract shall begin with an indication of the security classification of the information in the paragraph (unless the document itself is unclassified) represented as (S), (C), or (U). It is not necessary to include here abstracts in both offical languages unless the text is bilingual).

Two methods are presented for incorporating the effects of rough boundaries into propagation models based on the parabolic equation (PE) approximation. In particular, the acoustic scattering by a deterministically-rough, pressure-release surface is considered. In the first method, the vertical extent of the computational cell adjacent to the rough boundary is allowed to vary with range. This non-standard grid approach can readily be incorporated into existing finite-difference PE codes. In the second method, a low-impedance air-layer backing is appended to the rough surface and the original rough-surface scattering problem is replaced by one involving scattering from an internal, water/air interface. In this case, both finite-difference and split-step marching algorithms can be accommodated. Numerical results for the forward-scattered component of the field are provided for two benchmark problems.

14. KEYWORDS, DESCRIPTORS or IDENTIFIERS (technically meaningful terms or short phrases that characterize a document and could be helpful in cataloguing the document. They should be selected so that no security classification is required. Identifiers, such as equipment model designation, trade name, military project code name, geographic location may also be included. If possible keywords should be selected from a published thesaurus, e.g. Thesaurus of Engineering and Scientific Terms (TEST) and that thesaurus-identified. If it is not possible to select indexing terms which are Unclassified, the classification of each should be indicated as with the title.)

rough boundaries
propagation models
parabolic equation (PE)
pressure-release surface
finite-difference PE
air-layer backing
scattering
water/air interface
split-step PE
marching algorithms

#151186

NO. OF COPIES NOMBRE DE COPIES	COPY NO. COPIE N°	INFORMATION SCIENTIST'S INITIALS INITIALES DE L'AGENT D'INFORMATION SCIENTIFIQUE
1	1	JL

AQUISITION ROUTE / FOURNI PAR ▶ DREP

DATE ▶ 13 APRIL 1995

DSIS ACCESSION NO. / NUMÉRO DSIS ▶

DND 1158 (6-87)

National Defence / Défense nationale

PLEASE RETURN THIS DOCUMENT TO THE FOLLOWING ADDRESS:

DIRECTOR
SCIENTIFIC INFORMATION SERVICES
NATIONAL DEFENCE
HEADQUARTERS
OTTAWA, ONT. - CANADA K1A 0K2

PRIÈRE DE RETOURNER CE DOCUMENT À L'ADRESSE SUIVANTE:

DIRECTEUR
SERVICES D'INFORMATION SCIENTIFIQUES
QUARTIER GÉNÉRAL
DE LA DÉFENSE NATIONALE
OTTAWA, ONT. - CANADA K1A 0K2